Seventeenth International Conference on
Geometry, Integrability and Quantization
June 5–10, 2015, Varna, Bulgaria
Ivaïlo M. Mladenov, Guowu Meng
and Akira Yoshioka, Editors
Avangard Prima, Sofia 2016, pp 369–378
doi: 10.7546/giq-17-2016-369-378

Geometry, Integrability and Quantization XVII

AXIALLY SYMMETRIC WILLMORE SURFACES DETERMINED BY QUADRATURES

VASSIL M. VASSILEV*, PETER A. DJONDJOROV*, MARIANA TS. HADZHILAZOVA** and IVAÏLO M. MLADENOV**

**Institute of Mechanics, Bulgarian Academy of Sciences, Acad. G. Bonchev Str. Bl. 4, 1113 Sofia, Bulgaria*

***Institute of Biophysics, Bulgarian Academy of Sciences, Acad. G. Bonchev Str. Bl. 21, 1113 Sofia, Bulgaria*

Abstract. The work is concerned with a special family of axially symmetric surfaces providing local extrema to the so-called Willmore functional, which assigns to each surface its total squared mean curvature. The components of the position vector of the profile curves of the regarded Willmore surfaces satisfy a system of first-order ordinary differential equations. The solutions of this system are expressed by quadratures in terms of the tangent angle and, in this way, the corresponding Willmore surfaces are determined.

MSC: 34A05, 53A05, 74B20
Keywords: Analytic parametrization, ordinary differential equations, solutions by quadratures, Willmore surfaces

1. Introduction

The functional

$$\mathcal{W} = \int_{\mathcal{S}} H^2 \mathrm{d}A \tag{1}$$

which assigns to each surface $\mathcal{S}$ immersed in the three-dimensional Euclidean space its total squared mean curvature H, $\mathrm{d}A$ being the induced surface element, was proposed about two centuries ago by the prominent French scientists Siméon Denis Poisson and Marie-Sophie Germain as the bending energy of thin elastic shells [6, 9]. Nowadays, however, it is widely known as the Willmore functional (energy) due to the work [16] published in 1965 by the English geometer Thomas James Willmore (see also [17]).

The aforementioned note of T. J. Willmore attracted the interest of mathematicians to study the surfaces that provide local extrema to the functional (1) currently called "Willmore surfaces". These surfaces are determined by the solutions of the Euler-Lagrange equation corresponding to the Willmore functional, namely

$$\Delta H + 2(H^2 - K)H = 0 \tag{2}$$

where Δ is the Laplace-Beltrami operator on the surface $\mathcal{S}$ and K is its Gaussian curvature.

In the past four decades, the Willmore surfaces were studied by many authors both from purely mathematical point of view (see, e.g. [1, 7, 10] and references therein) and in the context of applications, for instance, in structural mechanics, biophysics and mathematical biology (see, e.g. [2, 7, 8, 11, 12]).

In this paper, which can be thought of as a continuation of our works [14, 15], we consider a special family of axially symmetric Willmore surfaces determined through a system of two first-order ordinary differential equations and express by quadratures the components of the position vector of the profile curves of the corresponding Willmore surfaces of revolution.

2. Axially Symmetric Willmore Surfaces

2.1. Axially Symmetric Surfaces

Denote by X, Y, Z the axes of a right-handed rectangular Cartesian coordinate system $\{x, y, z\}$ in $\mathbb{R}^3$. Consider an axially symmetric surface $\mathcal{S}$ in $\mathbb{R}^3$ obtained by revolving around the OZ-axis a plane curve Γ laying in the XOZ-plane. Then, without loss of generality, the components x, y, z of the position vector $\mathbf{x}$ of such a surface $\mathcal{S}$ can be given in the form

$$\mathbf{x}(t,\theta) = \begin{pmatrix} x(t,\theta) \\ y(t,\theta) \\ z(t,\theta) \end{pmatrix} = \begin{pmatrix} r(t)\cos\theta \\ r(t)\sin\theta \\ h(t) \end{pmatrix}, \qquad \theta \in [0, 2\pi], \qquad t \in \Omega \subseteq \mathbb{R} \tag{3}$$

where the functions $r(t)$ and $h(t)$ are supposed to have as many derivatives as may be required on the domain Ω. Let us remark that t is an arbitrary parameter along the curve Γ, i.e., the contour of the surface $\mathcal{S}$ at $\theta = 0$. In this notations, the first and second fundamental tensors of the surface $\mathcal{S}$ read

$$g_{\alpha\beta} = \begin{pmatrix} r_t^2 + h_t^2 & 0 \\ 0 & r^2 \end{pmatrix}, \qquad b_{\alpha\beta} = \frac{1}{\sqrt{r_t^2 + h_t^2}} \begin{pmatrix} r_t h_{tt} - h_t r_{tt} & 0 \\ 0 & r h_t \end{pmatrix} \tag{4}$$

respectively, and

$$g = \det(g_{\alpha\beta}) = r^2\left(r_t^2 + h_t^2\right), \qquad \mathrm{d}A = \sqrt{g}\,\mathrm{d}\theta\mathrm{d}t = r\sqrt{r_t^2 + h_t^2}\,\mathrm{d}\theta\mathrm{d}t. \tag{5}$$

Here and in what follows, the sub-indexes indicate derivatives with respect to the respective variable.

Consequently, the mean and Gaussian curvatures of the regarded surface read

$$H = \frac{1}{2}\frac{r\left(r_t h_{tt} - h_t r_{tt}\right) + h_t\left(r_t^2 + h_t^2\right)}{r\left(r_t^2 + h_t^2\right)^{3/2}} \tag{6}$$

$$K = \frac{z_t\left(r_t h_{tt} - h_t r_{tt}\right)}{r\left(r_t^2 + h_t^2\right)^2}. \tag{7}$$

2.2. Willmore Energy of Axially Symmetric Surfaces

On account of equations (5) and (6), the Willmore energy (1) of an axially symmetric surface $\mathcal{S}$ takes the form

$$\mathcal{W} = \int_\Omega \mathcal{L}\mathrm{d}t \tag{8}$$

where

$$\mathcal{L} = 2\pi\left[\frac{r\left(r_t h_{tt} - h_t r_{tt}\right) + h_t\left(r_t^2 + h_t^2\right)}{2r\left(r_t^2 + h_t^2\right)^{3/2}}\right]^2 r\sqrt{r_t^2 + h_t^2}. \tag{9}$$

2.3. Euler-Lagrange Equations

The application of the Euler operators

$$E_r = \frac{\partial}{\partial\, r} - D_t\frac{\partial}{\partial\, r_t} + D_t D_t\frac{\partial}{\partial\, r_{tt}} - \cdots$$

$$E_h = \frac{\partial}{\partial\, h} - D_t\frac{\partial}{\partial\, h_t} + D_t D_t\frac{\partial}{\partial\, h_{tt}} - \cdots$$

where

$$D_t = \frac{\partial}{\partial\, t} + r_t\frac{\partial}{\partial\, r} + h_t\frac{\partial}{\partial\, h} + r_{tt}\frac{\partial}{\partial\, r_t} + h_{tt}\frac{\partial}{\partial\, h_t} + \cdots$$

is the total differentiation operator, on the Lagrangian density $\mathcal{L}$ of the functional (8) leads to the Euler-Lagrange equations $E_r\mathcal{L} = 0$ and $E_h\mathcal{L} = 0$. However, it turned out that $r_t E_r\mathcal{L} \equiv -h_t E_h\mathcal{L}$ and hence we have a single equation determining the extremals of the Willmore energy (8), say

$$E_r\mathcal{L} = 0 \tag{10}$$

instead of a system of two Euler-Lagrange equations for two dependent variables $r(t)$ and $h(t)$ as expected. In other words, we have obtained an underdetermined system and to complete it we may add another equation of our own choice to equation (10). Three such cases are considered below.

First, assume

$$r_t^2 + h_t^2 = 1. \tag{11}$$

This means that t is the arc length s along the contour curve Γ. Then, in terms of the tangent angle φ we have

$$\dot{r} = \cos\varphi, \qquad \dot{h} = \sin\varphi \tag{12}$$

and can rewrite equation $E_r\mathcal{L} = 0$ in the form

$$\dddot{\varphi} = -\frac{2\cos\varphi}{r}\ddot{\varphi} - \frac{1}{2}\dot{\varphi}^3 + \frac{3\sin\varphi}{2r}\dot{\varphi}^2 + \frac{2 - 3\sin^2\varphi}{2r^2}\dot{\varphi} - \frac{\left(\cos^2\varphi + 1\right)\sin\varphi}{2r^3} \tag{13}$$

where the dots indicate derivatives with respect to the arc length s. At the same time, the expressions (6) and (7) for the mean and Gaussian curvatures take the familiar form

$$H = \frac{1}{2}\left(\dot{\varphi} + \frac{\sin\varphi}{r}\right), \qquad K = \dot{\varphi}\frac{\sin\varphi}{r}\cdot \tag{14}$$

Next, assume $t = h$ and denote $r = u(h)$. Then, equation (10) becomes

$$\begin{aligned}
&2u^3\left(u_h^2 + 1\right)^2 u_{hhhh}\\
&+4u^2u_h\left(u_h^2 + 1\right)\left(u_h^2 + 1 - 5uu_{hh}\right)u_{hhh}\\
&+5u^3\left(6u_h^2 - 1\right)u_{hh}^3 - 3u^2\left(u_h^2 + 1\right)\left(4u_h^2 - 1\right)u_{hh}^2\\
&-u\left(u_h^2 + 1\right)^2\left(2u_h^2 - 1\right)u_{hh} - \left(u_h^2 + 1\right)^3\left(2u_h^2 + 1\right) = 0.
\end{aligned} \tag{15}$$

It should be remarked that a variety of boundary value problems for Willmore surfaces of revolution have been studied recently on the ground of equation (15), see e.g. [3–5, 11, 12] and references therein.

Finally, assume $t = r$ and denote $h = w(r)$. In this case, equation (10) takes the form

$$\begin{aligned}
&2r^3\left(w_r^2 + 1\right)^2 w_{rrrr}\\
&+4r^2(w_r^2 + 1)(w_r^2 + 1 - 5rw_rw_{rr})w_{rrr}\\
&+5r^3(6w_r^2 - 1)w_{rr}^3 - 15r^2w_r(w_r^2 + 1)w_{rr}^2\\
&+r(w_r^2 + 1)(w_r^2 - 2)w_{rr} + w_r(w_r^2 + 1)^3(w_r^2 + 2) = 0
\end{aligned} \tag{16}$$

and the mean and Gaussian curvatures read

$$H = \frac{1}{2r}\frac{rw_{rr} + w_r^3 + w_r}{(1 + w_r^2)^{3/2}}, \qquad K = \frac{1}{r}\frac{w_{rr}w_r}{(1 + w_r^2)^2}\cdot \tag{17}$$

Note that the mappings

$$w \to -w, \qquad w \to w + \omega, \qquad w \to w\eta, \qquad r \to r\eta, \qquad \omega, \eta \in \mathbb{R} \tag{18}$$

transform one solution of equation (16) into another, i.e. one axisymmetric Willmore surface determined in this way into another one obtained from it by reflection about the XOY-plane or scaling of the respective position vector.

3. A Particular Family of Willmore Surfaces of Revolution

3.1. Determining Equations

It was established in [13] that each solution of the following normal system of two ordinary differential equations

$$\frac{\mathrm{d}w}{\mathrm{d}r} = v, \qquad \frac{\mathrm{d}v}{\mathrm{d}r} = \frac{1}{r}\left(v^2+1\right)\sqrt{v^2 + 2\,\alpha\sqrt{v^2+1}}, \qquad \alpha \in \mathbb{R} \tag{19}$$

satisfies equation (16) and hence determines a Willmore surface of revolution. Indeed, taking into account that the above system is equivalent to the single second-order equation

$$\frac{\mathrm{d}^2 w}{\mathrm{d}r^2} = \frac{1}{r}\left[\left(\frac{\mathrm{d}w}{\mathrm{d}r}\right)^2 + 1\right]\sqrt{\left(\frac{\mathrm{d}w}{\mathrm{d}r}\right)^2 + 2\,\alpha\sqrt{\left(\frac{\mathrm{d}w}{\mathrm{d}r}\right)^2+1}} \tag{20}$$

and substituting the expressions for the derivatives w_{rr}, w_{rrr} and w_{rrrr} obtained from equation (20) into the left-hand side of equation (16) one can verify that it equals zero.

Substituting equations (19) into equations (17) one obtains the following expressions for the mean and Gaussian curvatures of a surface belonging to the regarded family of axially symmetric Willmore surfaces

$$H = \frac{v + \sqrt{v^2 + 2\,\alpha\sqrt{v^2+1}}}{2r\sqrt{v^2+1}}, \qquad K = \frac{v\sqrt{v^2 + 2\,\alpha\sqrt{v^2+1}}}{r^2\left(v^2+1\right)} \tag{21}$$

where $v = v(r)$ should satisfy the second equation of system (19).

3.2. Parametrization by Quadratures

Evidently, system (19) can be cast in the form

$$\begin{aligned} \frac{\mathrm{d}r}{\mathrm{d}v} &= \frac{r}{\left(v^2+1\right)\sqrt{v^2+2\alpha\sqrt{v^2+1}}} \\ \frac{\mathrm{d}w}{\mathrm{d}v} &= \frac{vr}{\left(v^2+1\right)\sqrt{v^2+2\alpha\sqrt{v^2+1}}} \end{aligned} \tag{22}$$

in which v plays the role of the independent variable while r and w are regarded as dependent variables. It is straightforward to present the solutions of system (22) by quadratures, namely

$$
\begin{aligned}
r(v) &= c_1 \exp\left[\rho(v)\right] \\
w(v) &= c_1 \int \frac{\exp\left[\rho(v)\right] v \, \mathrm{d}v}{(v^2+1)\sqrt{v^2 + 2\,\alpha\sqrt{v^2+1}}} + c_2
\end{aligned}
\tag{23}
$$

where c_1 and c_2 are arbitrary real numbers and

$$
\rho(v) = \int \frac{\mathrm{d}v}{(v^2+1)\sqrt{v^2 + 2\,\alpha\sqrt{v^2+1}}} \cdot \tag{24}
$$

Thus, the axially symmetric Willmore surfaces belonging to the considered family are parametrized analytically in terms of the parameter v, which is nothing but the tangent of the slope angle.

It can be proved that each solution of system (22) is real-valued and bounded provided that $v \in (-\infty, \infty)$ if $\alpha > 0$ and $v \in (-\infty, -\varepsilon)$ or $v \in (\varepsilon, +\infty)$, where $\varepsilon = \sqrt{2\alpha^2 + 2\sqrt{\alpha^2 + \alpha^4}}$, if $\alpha < 0$. In the case $\alpha = 0$ one obtains only spheres and catenoids, see [13, p. 259].

4. Numerical Results

In this study, the integrals on the right-hand sides in formulas (23) and (24) are computed numerically. The expression (24) can be written in the form

$$
\rho(v) = \int_a^b \frac{\mathrm{d}\tau}{(\tau^2+1)\sqrt{\tau^2 + 2\,\alpha\sqrt{\tau^2+1}}} \tag{25}
$$

where a and b $(a \leq b)$ are chosen appropriately for each case considered here and the integral is computed by the routine `NIntegrate` in *Mathematica*®. The second expression in (23) is written in the form

$$
w(v) = \int_a^b \frac{\tau\, r(\tau)\, \mathrm{d}\tau}{(\tau^2+1)\sqrt{\tau^2 + 2\,\alpha\sqrt{\tau^2+1}}} \tag{26}
$$

and in order to avoid nested `NIntegrate` routines, this integral is computed in the following manner: the interval $[a, b]$ is divided in n subintervals of equal length $\Delta\tau = (b-a)/n$ and the expression (26) is computed numerically using the midpoint approximation, namely

$$
w(v) = \sum_{\tau=1}^{n} \Delta\tau \frac{\tilde{\tau}\, r(\tilde{\tau})}{(\tilde{\tau}^2+1)\sqrt{\tilde{\tau}^2 + 2\,\alpha\sqrt{\tilde{\tau}^2+1}}}, \qquad \tilde{\tau} = \tau + \frac{\Delta\tau}{2} \tag{27}
$$

where for each $\tilde{\tau}$, $r(\tilde{\tau}) = \mathrm{e}^{\rho(\tilde{\tau})}$ is computed using `NIntegrate` as is mentioned above.

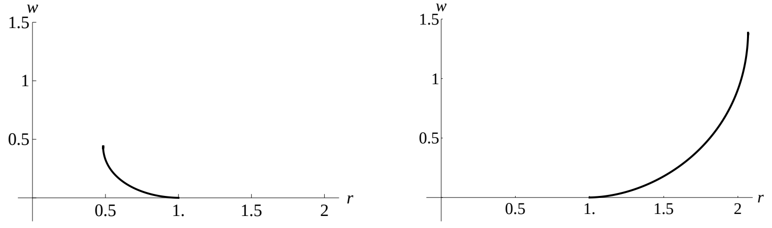

Figure 1. Parametric plots of two distinct shapes, provided by the expressions (25), (26) for $\alpha = 1$: the curve to the left corresponds to $v \in (-\infty, 0]$, and the curve to the right – to $v \in [0, \infty)$.

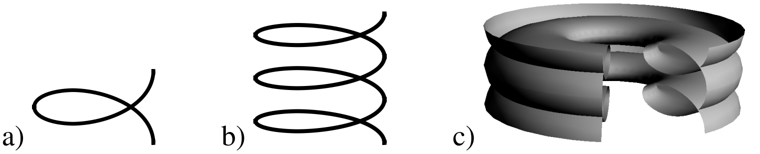

Figure 2. Parametric plots of a fragment of a nodoid-like profile a), and samples of the corresponding profile curve b), and surface c) for $\alpha = 1$.

In the case $\alpha > 0$, the root in the right-hand side of the second equation (19) is real for $-\infty < v < \infty$ and formulas (25), (26) imply

$$r(0) = 1, \qquad w(0) = 0. \tag{28}$$

In fact, the expressions (25), (26) comprise two distinct fragments in (r, w)-plane, corresponding to positive or negative values of v, respectively. The boundaries of the integrals (25), (26) are chosen to be $a = 0$, $b = v$ for the positive values of v and $a = v$, $b = 0$ for the negative ones. A particular example of such fragments is shown in Fig. 1.

Using appropriate transformations of form (18) of these two fragments, one can construct a variety of profile curves that are smooth solutions to system (19).

Indeed, using the reflection $w \to -w$ and translation one obtains the fragment shown in Fig.2a). Reflecting and translating appropriately this fragment one gets the profile curve (see Fig.2b)), which gives rise to the nodoid-like surface shown in Fig.2c).

In the case $\alpha < 0$ the formulas (28) do not hold any more; see the note at the end of subsection 3.2. In this case, expressions (25), (26) give rise to another couple of curves in (r, w)-plane, one of which is obtained for negative values of v and the boundaries of the integrals (25), (26) are $a = v$, $b = \varepsilon$, whereas the other one is obtained for positive values of v and $a = \varepsilon$, $b = v$. A particular example of such fragments is shown in Fig.3. As in the previous case, transforming these two

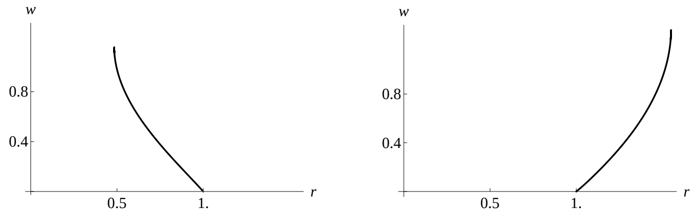

Figure 3. Parametric plots of the two shapes, provided by expressions (25), (26) for $\alpha = -0.5325$: the curve to the left corresponds to $v \in (-\infty, -\epsilon)$, and the curve to the right – to $v \in (\epsilon, \infty)$.

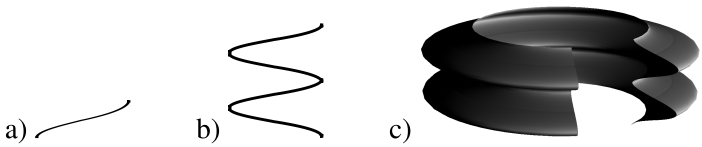

Figure 4. Parametric plots of a fragment of a unduloid-like profil a), and samples of the corresponding profile curve b), and surface c) for $\alpha = -1$.

curves by means of the mappings (18) one can plot a fragment of a profile curve, which corresponds to the unduloid-like surface shown in Fig.4.

Finally, it is possible co combine profile curves corresponding to various values of α in order to obtain a smooth axially symmetric Willmore surface, provided that the curvatures at the contact points are continuous. Indeed, the two fragments in Fig.1 can be combined into the profile, shown in Fig.5a). Combining it with the fragment shown in Fig.4a) one obtains the smooth profile curve Fig.5b), giving raise to the surface depicted in Fig.5c).

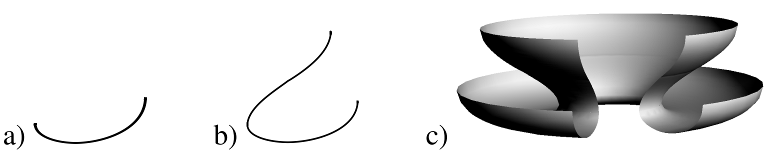

Figure 5. Parametric plots of: a) a fragment of a nodoid-like profile, b) a combination of the curve in Fig.4a) and this fragment, c) the corresponding surface.

5. Concluding Remarks

This work studies the Willmore surfaces in revolution. It is established that the system of Euler-Lagrange equations associated with the corresponding variational

problem (8), (9) is underdetermined. Three types of well-known ordinary differential equations (12) - (13), (15) and (16) describing such surfaces are shown to come out of this variational formulation.
Then, a special family of axially symmetric Willmore surfaces are studied – those determined by the system of two first-order ordinary differential equations (19). A closed form solution by quadratures of form (23) to equations (19) is derived using a parametrization of form $r(v)$, $w(v)$, where (r, w) is the position vector and v is the tangent of the slope angle of the respective profile curve. This solution gives rise to three sorts of Willmore surfaces of revolution, namely nodoid-like, unduloid-like and the one presented in Figs. 2, 4 and 5, respectively.

Achnowledgements

This research is within the project under the auspices of the Bilateral Agreement between Bulgarian and Polish Academy of Sciences.

References

[1] Athukoralage B., Aulisa E., Bornia G. and Toda M., *New Advances in the Study of Generalized Willmore Surfaces and Flow*, Geom. Integrability & Quantization **17** (2016) 133–142.

[2] Castro-Villarreal P. and Guven J., *Axially Symmetric Membranes with Polar Tethers* Journal of Physics A: Math. & Theor. **40** (2007) 4273–4283.

[3] Dall'Acqua A., Fröhlich S., Grunau H.-Ch. and Schieweck F., *Symmetric Willmore Surfaces of Revolution Satisfying Arbitrary Dirichlet Boundary Data*, Preprint 24-2008, Faculty of Mathematics, University of Magdeburg, Magdeburg 2008.

[4] Dall'Acqua A., Deckelnick K. and Grunau H.-Ch., *Classical Solutions to the Dirichlet Problem for Willmore Surfaces of Revolution*, Advances in Calculus of Variations **4** (2008) 379–397.

[5] Dall'Acqua A., Deckelnick K. and Wheeler G. *Unstable Willmore Surfaces of Revolution Subject to Natural Boundary Conditions*, Calculus of Variations and Partial Differential Equations **48** (2013) 293–313.

[6] Germain S., *Recherches sur la théorie des surfaces élastiques*, Veuve Courcier, Paris 1821.

[7] Grunau H.-Ch., *Nonlinear Questions in Clamped Plate Models*, Milan J. Math. **77** (2009) 171–204.

[8] Jülicher F. *The Morphology of Vesicles of Higher Topological Genus*: *Conformal Degeneracy and Conformal Modes*, J. Phys. II France **6** (1996) 1797–1924.

[9] Poisson S., *Mémoire sur les surfaces élastiques*, Mem. Cl. Sci. Math. Phys., Inst. de France (1812) 167–225.

[10] Rivière T., *Analysis Aspects of Willmore Surfaces*, Inventiones Mathematicae **174** (2008) 1-45, doi: 10.1007/s00222-008-0129-7.

[11] Toda M. and Athukoralage Bh., *Geometry of Biological Membranes and Willmore Energy*, AIP Conf. Proc. **1558** (2013) 883–886.

[12] Toda M. and Athukorallage B., *Geometric Models for Secondary Structures in Proteins*, Geom. Integrability & Quantization **16** (2015) 282–300.

[13] Vassilev V. and Mladenov I., *Geometric Symmetry Groups, Conservation Laws and Group-Invariant Solutions of the Willmore Equation*, Geom. Integrability & Quantization **5** (2004) 246–265.

[14] Vassilev V., Djondjorov P., Hadzhilazova M. and Mladenov I., *Analytic Representation of a Class of Axially Symmetric Willmore Surfaces*, In: Integrability, Recursion Operators and Soliton Interactions, B. Aneva, G. Grahovski, R. Ivanov and D. Mladenov (Eds), Avangard Prima, Sofia 2014, pp. 325–330.

[15] Vassilev V., Djondjorov P., Atanassov E., Hadzhilazova M. and Mladenov I., *Explicit Parametrizations of Willmore Surfaces*, AIP Conf. Proc. **1629** (2014) 201–206.

[16] Willmore T., *Note on Embedded Surfaces*, An. Ştiinţ. Univ. "Al. I. Cuza" Iaşi Se çt. Ia Mat. **11** (1965) 493–496.

[17] Willmore T., *Riemannian Geometry*, Oxford University Press, Oxford 1993.